Journal of Applied Polymer Science

Hyperelasticity, dynamic mechanical property, and rheology of addition-type silicone rubber (VPDMS cured by PMHS)

Dong Hao, Dongxu Li, Yihuan Liao
College of Aerospace Science and Engineering, National University of Defense Technology, No. 47, Sanyi Street, Changsha 410073, People's Republic of China
Correspondence to: D. Hao (E-mail: haodong@nudt.edu.cn)

ABSTRACT: The aerospace-level addition-type silicone rubber (ASR) was prepared by vinyl-terminated polydimethylsiloxane (VPDMS) and aerospace-level polymethylhydrosiloxane (PMHS) and its mechanical properties were investigated through the hyperelastic measurements, the dynamic mechanical tests and the rheological experiments. The hyperelastic analysis shows that the tensile strength and the break strain are separately 3.00 MPa and 281%, and the proposed model exhibits good descriptions of the uniaxial behaviors. The dynamic mechanical analysis indicates that two transition temperatures are observed for the ASR. The storage modulus, the loss modulus and the loss factor become stable when the temperature is higher than −35°C. The rheological analysis presents that the storage and loss modulus appeared an obvious growth with increasing frequency at the temperature of −120 and −110°C. The moduli have an apparent nonlinear dependence on the strain amplitude and a nonlinear function is utilized to express that relationship. This nonlinear model shows well agreements with the experimental data. The investigations on the aerospace-level ASR in this article have some meanings for its usage in aerospace products. © 2015 Wiley Periodicals, Inc. J. Appl. Polym. Sci. **2015**, *132*, 42036.

KEYWORDS: addition polymerization; crosslinking; elastomers; mechanical properties; properties and characterization

Received 31 August 2014; accepted 26 January 2015
DOI: 10.1002/app.42036

INTRODUCTION

Silicone rubbers, which have the unique structure of polysiloxane, exhibit a list of excellent characteristics including biocompatibility, thermal stability, oxidation resistance, climate resistance and so on.[1–14] They have considerable commercial importance and have been widely used in industrial applications. In recent years, with the development of aerospace industry, silicone rubbers start to be used in aerospace field. Different from the usage in generally industrial applications, the silicone rubbers employed in aerospace applications must satisfy the aerospace requirement (such as low mass loss and low gas leakage) and have stable mechanical properties. So far, there have been just few publications for the aerospace-level ASR. In this article, we mainly focus on the investigations on the aerospace-level ASR, and this study would play a significant role in its aerospace applications and industrial applications.

The purpose of this article is (i) to propose a model expressing and analyzing the hyperelasticity of the ASR, and (ii) to study the dynamic mechanical properties and the rheological behaviors of the ASR.

In hyperelastic investigations, many theoretical models were reported to express the hyperelasticity of the rubber-like materials,[15–18] such as Nunes model,[1] Yeoh model,[19] and Exp-Ln model.[20] However, these models may be suitable for some certain materials, not all the materials. In this article, a model is reduced from Lopez-Pamies's model[21] and the hyperelasticity of the ASR was studied based on the reduced model.

Many experiments have been carried out to investigate the mechanical properties of the silicone rubbers. The mechanical properties of the silicone rubber/polyurethane/epoxy blends and the silicone rubber/polyacrylate blends were tested by Wang *et al.*,[6] and Chiu *et al.*,[22] respectively. The mechanical behaviors of the starch/silicone oil/silicone rubber blends were reported by Hao *et al.*,[10] whose materials were the commercial room temperature vulcanization rubber. Chen *et al.*, adopted the divinyl-hexa[(trimethoxysilyl)ethyl]-POSS as the crosslinker to prepare the room temperature vulcanization silicone rubber.[11] The poly(vinylidene fluoride)/silicone rubber blends were manufactured and tested by Wang *et al.*[23,24] The effect of the temperature on the mechanical behaviors of the unfilled and filled silicone rubbers were investigated by Rey *et al.*,[25] but the influence of the frequency and the strain amplitude was not considered. Guelon *et al.*, designed a new testing system for the purpose of investigating the rubber's mechanical behaviours.[26] Zinc dimethacrylate was used to work as the

Table I. Physical Properties of VPDMS and PMHS

Physical property	VPDMS	PMHS
Appearance	Ivory-white and semilucent	Transparent
Density (g cm^{-3}, 25°C)	1.1	0.98
Viscosity (Pa s, 25°C)	33	0.03
Mixing mass ratio	100	4

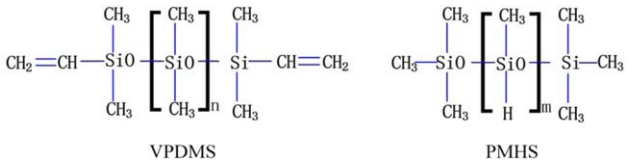

Figure 1. Chemical structural formulas of VPDMS and PMHS. [Color figure can be viewed in the online issue, which is available at wileyonlinelibrary.com.]

cured agent by Meng *et al.*[27] The compression experiments of the silicone rubbers were carried out by Vesenjak *et al.*,[28] but the dynamic mechanical and rheology tests were not taken into account. The influence of $-CH_2CH_2CF_3$ on the mechanical properties of VPDMS and the influence of $Ph_{12}SQ$ on the mechanical properties of polydimethylsiloxane (PDMS) were separately researched by Li *et al.*,[29] and Moghadam *et al.*[30] The experimental investigation on dynamic properties of rubbers were done by Weia *et al.*[31] and Ramorino *et al.*[32] A detailed review on silicone rubbers was reported by Shit Pathik Shah.[33]

Recently, the vulcanization technology of the ASR (VPDMS cured by PH) was studied by Zhang *et al.*[34] and the modified PMHS was prepared by Li *et al.*[35] But they focused on the curing technology and the ingredient of the ASR, and the mechanical properties of the ASR, which are important for its future industrial or aerospace applications were not given.

Although numerous investigations on the silicone rubber have been published, few of them employed the raw materials, which have been or will be used in aerospace applications. With respect to these studies, they aimed at commercial materials, while we pay attention to aerospace level materials. Different from the aforementioned studies, in this article we investigated the hyperelasticity, the dynamic mechanical properties, and the rheology of the ASR for its possible usage in space. The aerospace-level raw materials of VPDMS and PMHS were employed and the ASR was prepared by the curing technology from the manufacturer. The investigations on the mechanical behaviors of the aerospace-level ASR are necessary for its applications.

Summing up, the purposes of this article are (i) to prepare the aerospace-level ASR that will be utilized in aerospace products, (ii) to investigate the hyperelasticity of the ASR by three theoretical models and the uniaxial tests, (iii) to study the dynamic mechanical properties by the dynamical mechanical analysis, (iv) to research the rheological behaviors through the frequency sweep test and the strain amplitude sweep test. The material preparation procedures and the related experiments are described in Experimental section. Results and discussion section presents the results and discussion of the ASR. Some conclusions close the article.

EXPERIMENTAL

Materials

The raw materials that put into use in this article are two-componential liquid silicone rubbers: one component is VPDMS and the other component is PMHS. The aerospace-level raw materials of VPDMS and PMHS were purchased from Chenguang Chemical Research Institute (Sichuan, China). The uncured silicone is VPDMS. PMHS works as the crosslinking agent as it contains active Si—H bonds. The physical properties of VPDMS and PMHS are listed in Table I. The chemical structural formulas of VPDMS and PMHS are sketched in Figure 1. More detailed information about the aerospace-level ASR was not obtained from the manufactures.

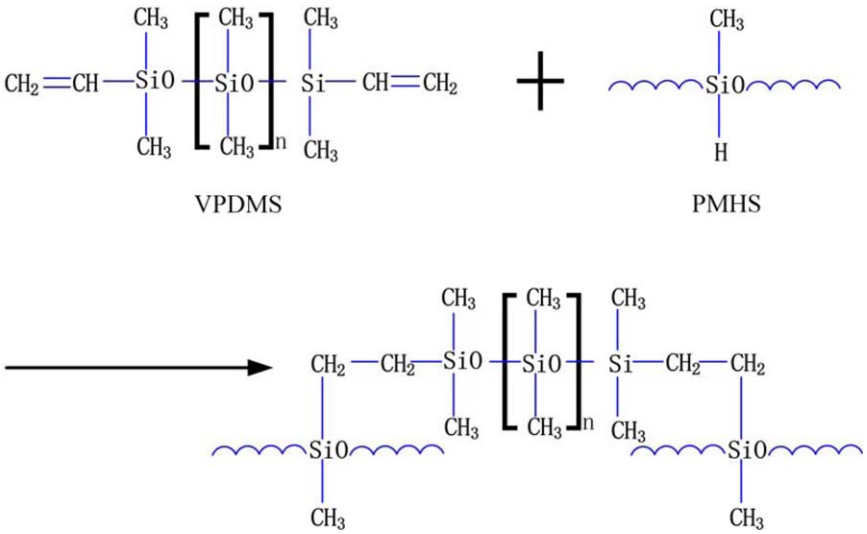

Figure 2. Crosslinking reaction between VPDMS and PMHS. [Color figure can be viewed in the online issue, which is available at wileyonlinelibrary.com.]

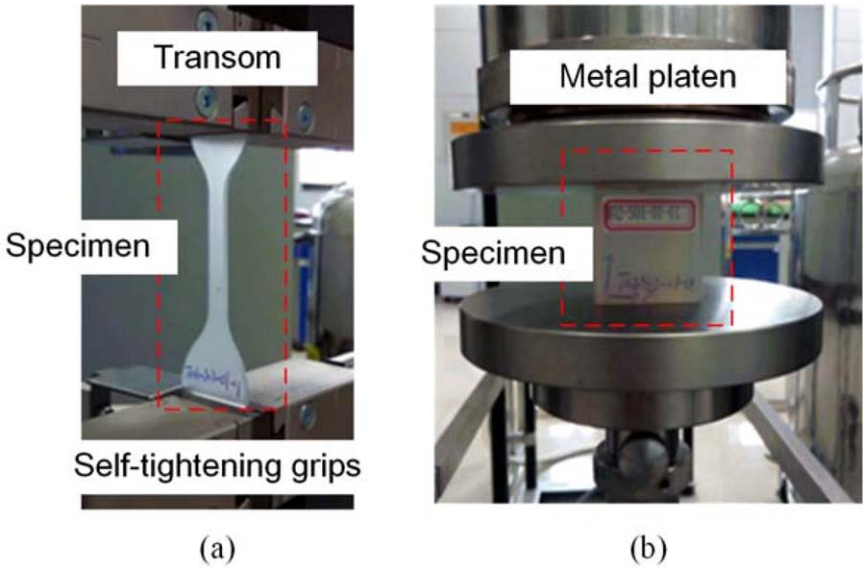

Figure 3. Hyperelastic measurements: (a) uniaxial tension, (b) simple compression. [Color figure can be viewed in the online issue, which is available at wileyonlinelibrary.com.]

Preparation of Silicone Rubber

The unique recommendatory vulcanization technology was adopted. This vulcanization technology is supplied by the manufacturer. The detailed vulcanization operations are given as follows.

First, VPDMS and PMHS were mixed with a 100/4 mass ratio. Second, the uncured mixture was stirred in a vacuum stirrer for 30 min to eliminate the undesirable entrapped bubbles and obtain a uniform liquid-like mixture. Third, the liquid uncured mixture was injected into the molds. Fourth, the molds were put in an open environment for 1440 min to cure the mixture at room temperature, which allows the uncured mixture to undergo a condensation reaction (Figure 2). As can been in Figure 2, when PMHS is used as curing agent, there does not generate any small molecule when crossing-linking reaction occurs. That character assures the low total mass loss (TML). The used molds are made of aluminum alloy and their inner surfaces have been coated with a chromium layer. Fifth, the mold-release operations were carried out after the mixture was cured at room temperature. Finally, the mold-released blends were put inside an oven at 100°C for 360 min to undergo the secondarily curing process. To perform the experiments conveniently, the cured ASR was trimmed to a proper size. The density of the cured ASR is 1.07 g cm^{-3} and the shore hardness is 37 A.

Hyperelastic Measurements

Since, in many scenes, the silicone rubber components usually work under the uniaxial stress state,[3] the mechanical property of the uniaxial deformation is more important than that of other deformation modes. The uniaxial tests have been standardized at national and international level.[36] The uniaxial tests were also performed by Bradley *et al.*, to investigate the rubber's elasticity.[37] In this article, the uniaxial tests (including uniaxial tension and simple compression) were performed by a universal mechanical testing machine (Zwick Z010, 1 kN, Germany) at room temperature. To avoid the relative slip between the specimen and the extensometer, the measured displacement of the transom or platen (Figure 3) was utilized to compute the stretch for the uniaxial tests.

The uniaxial tension tests were carried out on the dumbbell shaped samples at room temperature. The dumbbell shaped specimens were manufactured according to GB/T 528–2009. The tested specimen was held in self-tightening grips as presented in Figure 3(a). The tension specimen was extruded at a speed of 500 mm min^{-1} until it teared.[15,37] The uniaxial tension tests were performed on three specimens and the results were averaged to diminish the measurement error.

The simple compression tests were performed on the cubic-shaped specimens with the size of 40 × 23.75 × 39.5 mm^3, because the cubic-shaped structures were widely used in engineering applications. The dimension of the compression direction was 39.5 mm. The tests were implemented according to GB/T 7757-2009. The specimen was fixed between two metal platens, as seen in Figure 3(b). The absolute displacement of the simple compression tests was much smaller than that of the uniaxial tension tests, therefore, a much smaller compression speed was required for obtaining stable measurement data. In the present article, the specimens were compressed at a speed of 10 mm min^{-1} until the compression amount reached 50%.[36] The uniaxial compression tests were also carried out on three specimens and the measured results of the three specimens were averaged to be the final experimental data.

Dynamic Mechanical Test

For the purpose of using the ASR as damping materials, the dynamic mechanical behavior should be determined by a dynamic viscoelastometer (EPLEXOR 500N/1500N, GABO QUALIMETER Testanlagen GmbH, Germany). The dynamic mechanical test was carried out with tension deformation mode at 5 Hz. The heating rate was set as 2°C min^{-1} and the

Table II. Nominal Stress Expressions

Model	Nominal stress	Coefficients
Nunes	$f=\left(1-\lambda^{-3}\right)\left(C_1\lambda+\frac{3}{4}C_2\left(\lambda^{-2}+2\lambda-3\right)^{-1/4}\right)$	C_1, C_2
Yeoh	$f=2\left[C_{10}+2C_{20}\left(\lambda^2+2/\lambda-3\right)\right]\left(\lambda-\frac{1}{\lambda^2}\right)$	C_{10}, C_{20}
Proposed	$f=2C\left(\lambda-\lambda^{-2}\right)\left(2\lambda^{-1}+\lambda^2\right)^{\alpha-1}$	C, α

f is the nominal stress and λ is the stretch.

temperature range was set from −130 to 150°C. The static strain amplitude and the dynamic strain amplitude were separately set as 1% and 0.1%. The sample was prepared as a cut strip with the size of 20 × 6 × 2.4 mm^3 for the temperature scanning test. Therefore, the relationships among the storage modulus (E'), the loss modulus (E''), the damping factor (tanδ) and the temperature could be obtained.

Rheological Characterization

To further understand the mechanical properties of the ASR, the rheological experiments were also carried out by the dynamic viscoelastometer. The rheological tests were performed in both frequency sweep mode and strain amplitude sweep mode. The frequency sweep test was carried out with tension deformation mode. The frequency scanning range is from 0.5 to 15 Hz. The static strain amplitude was set as 1% and the dynamic strain amplitude was set as 0.1%. The temperature range in the frequency sweep test was set from −120 to 20°C. The strain amplitude sweep test was carried out at 20°C and performed with double-shear mode. The amplitude sweep range is set from 0 to 20% and the vibration frequency of 5 Hz was adopted. Then, the relationships among the shear storage modulus (G'), the shear loss modulus (G''), the damping factor (tanδ) and the shear strain amplitude could be obtained.

RESULTS AND DISCUSSION

Hyperelastic Models and Analysis

According to the measured results, the tensile strength and the break strain of the ASR are separately 3.00 MPa and 281%. The tensile strength and the break strain are small, and the ASR components in our study will be used to work under compression deformation state. Thus, the relationship between the nominal stress and the stretch of the uniaxial deformation case is still meaningful to the engineering applications of the ASR. The ASR can be classified as hyperelastic materials, which allow largely reversible deformations in the rubber region. To study this hyperelastic behavior, a function so-called strain energy density function (SEDF) is usually utilized.[38] There have been many proposed SEDFs and the most widely cited one is Mooney-Rivlin model for its simplicity.[1] Since Mooney-Rivlin model sometimes cannot describe the nonlinear behavior, Yeoh model is sometimes adopted.[19] Yeoh model has two parameters and it is given as follows:

$$W_{\text{Yeoh}}=C_{10}(I_1-3)+C_{20}(I_1-3)^2 \tag{1}$$

where C_{10} and C_{20} are the material parameters.

In addition, Nunes developed Mooney-Rivlin model and used it to investigate the hyperelasticity of polydimethylsiloxane (PDMS). Nunes model is shown as follows:[1]

$$W_{\text{Nunes}}(I_1,I_2)=\frac{1}{2}\left[C_1(I_1-3)+C_2(I_2-3)^{3/4}\right] \tag{2}$$

where C_1 and C_2 are material constants; I_1 and I_2 are the strain invariants.[39] Nunes model could express the shear behavior of PDMS well, but may be not suitable for some other materials. So, in our study, a reduced SEDF is developed from Lopez-Pamies's model as follows:[21]

$$W_{\text{Proposed}}=\frac{C}{\alpha}(I_1{}^{\alpha}-3^{\alpha}) \tag{3}$$

where C and α are material parameters. When $\alpha=1$, the proposed SEDF degrades to neo-Hookean model.[40]

Nunes model, Yeoh model and the proposed model for the uniaxial deformation behavior are listed in Table II. Using the experimental data of the uniaxial tension test, the parameters in Nunes model, Yeoh model and the proposed one are identified by nonlinear least square method (NLSM). The results of the uniaxial tension and the simple compression experiments are displayed in Figures 4 and 5, respectively.

As illustrated in Figure 4, the fitted results of the proposed model for the uniaxial tension test are in better agreements with the experimental data than that of Nunes model and Yeoh model. The fitted results of Yeoh model are much better than that of Nunes model. Seeing from Figure 4, Nunes model overestimates the nominal stress when $\lambda<3$ and underestimates the

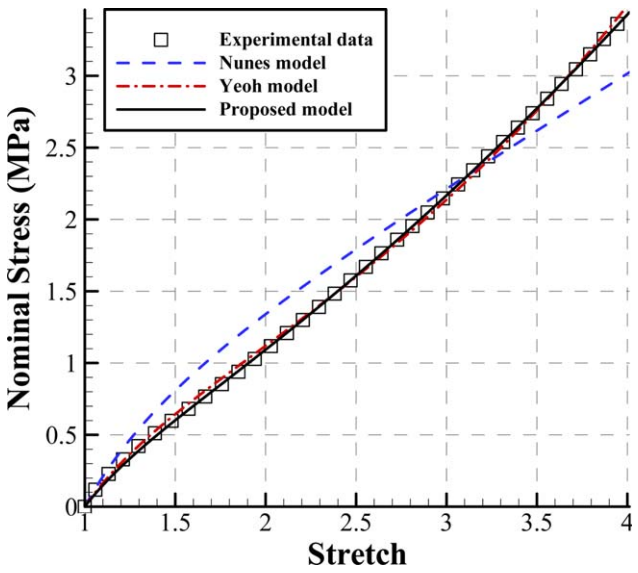

Figure 4. Fitted results of uniaxial tension test for ASR. [Color figure can be viewed in the online issue, which is available at wileyonlinelibrary.com.]

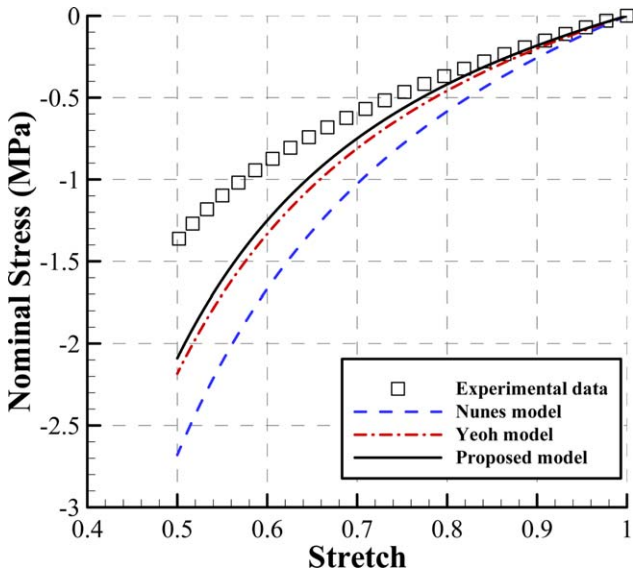

Figure 5. Predicted results of simple compression test for ASR using parameters identified by uniaxial tension data. [Color figure can be viewed in the online issue, which is available at wileyonlinelibrary.com.]

nominal stress when $\lambda > 3$. But for Yeoh model, it overestimates the nominal stress when $\lambda < 2$ and is as good as the proposed model when $\lambda > 2$. Figure 5 presents a comparison between the experimental data in simple compression and the predicted results of the three models aforementioned. The compared results show that for predicting the simple compression behavior, the proposed model performs best among these three models. When $0.9 < \lambda < 1$, both Yeoh model and the proposed model can predict the compression behavior of the ASR accurately, and perform better than Nunes model. When $\lambda < 0.9$, all these three models overestimate the nominal stress; however, the proposed model still performs better than the other two.

Summing up, the proposed model is suitable to describe the hyperelasticity of the aerospace-level ASR investigated in this article. It is worthy noting that, all these three models (Nunes model, Yeoh model and the proposed model) contain two material parameters, but the proposed model exhibits preferable descriptions of uniaxial hyperelastic behaviors for the ASR. Besides, there are no cracks in the outer edges of the specimens for the uniaxial compression experiment.

Dynamic Mechanical Analysis

The temperature dependences of the storage modulus E', the loss modulus E'' and the loss factor tanδ for the ASR are depicted in Figure 6. The temperature, corresponding to the maximum tanδ, is usually defined by the glass transition temperature. However, this definition may be not suitable for the ASR. The ASR presents two transition temperatures within the temperature range from −130 to 150°C: the first one is −115°C, which is related with the glass transition temperature T_g (close to HPDMS[15]) and the other one corresponds to the crystallization temperature T_c, lying between −50 and −35°C.

The loss factor tanδ at the temperature of T_g is 0.15123 and it increases rapidly in the temperature range from −50 to −35°C. The storage modulus and the loss modulus decrease three orders of magnitudes in that temperature range. In that crystallization temperature range, the macromolecular starts to change from the ordered state to the disordered state and the friction between macromolecules becomes larger. Larger friction may lead to larger damping. When the temperature is higher than −35°C, the loss factor tanδ fluctuates within the range from 0.24 to 0.37 and is larger than that at the glass transition temperature.

When the temperature is higher than −35°C, the storage modulus and the loss modulus of the ASR become stable and the loss factor tanδ is larger than 0.24, i.e., the ASR could be used as the excellent elastic and damping materials when the working temperature is between −35 and 150°C. And an unconspicuous decreasing trend for tanδ could also be observed.

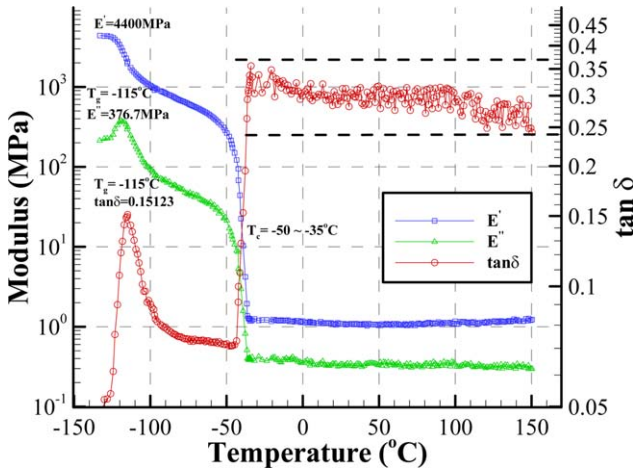

Figure 6. Effect of temperature on storage modulus, loss modulus and damping factor of ASR. [Color figure can be viewed in the online issue, which is available at wileyonlinelibrary.com.]

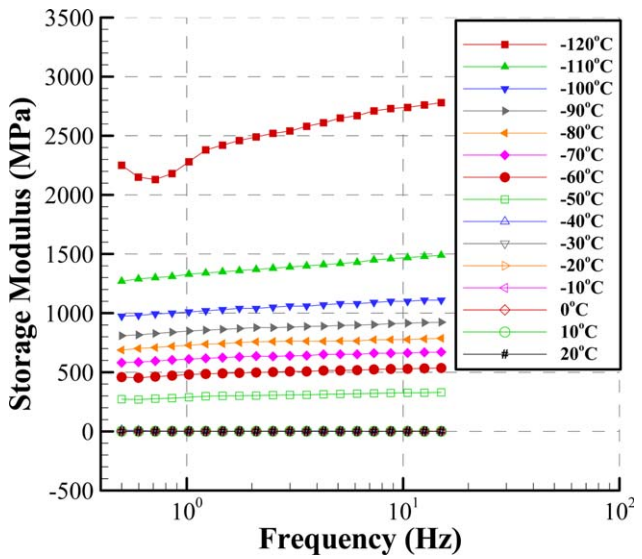

Figure 7. Storage modulus of ASR as a function of frequency. [Color figure can be viewed in the online issue, which is available at wileyonlinelibrary.com.]

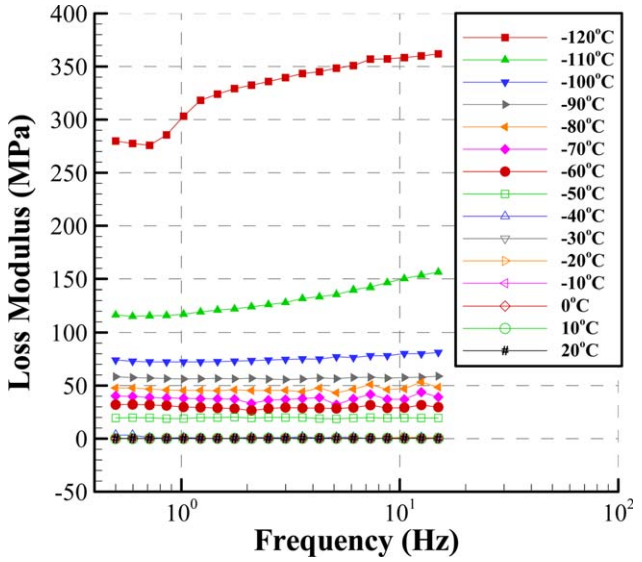

Figure 8. Loss modulus of ASR as a function of frequency. [Color figure can be viewed in the online issue, which is available at wileyonlinelibrary.com.]

Rheology Analysis

The relationships among the storage modulus, the loss modulus and the frequency at the static strain amplitude of 1% and the dynamic strain amplitude of 0.1% within the temperature range from −120 to 20°C, are given in Figures 7 and 8, respectively. The frequency sweep test was performed in the linear viscoelastic region. Polymers are of non-Newtonian nature and their viscosity is complicated.[41,42] However, at the temperature of −120 and −110°C, with increasing frequency, storage modulus and loss modulus appeared an obvious growth.

The storage modulus changes from 2250 to 2700 MPa at −120°C and from 1250 to 1400 MPa at −110°C. The loss modulus varies from 280 to 360 MPa at −120°C and from 115 to 160 MPa at −110°C. Furthermore, the storage modulus is one order of magnitude larger than the loss modulus. This phenomenon indicates that the ASR may have excellent elastic behavior. When the temperature varies from −40 to 20°C, the curves of modulus are close to each other. The storage modulus and the loss modulus become stable when the temperature is higher than −40°C.

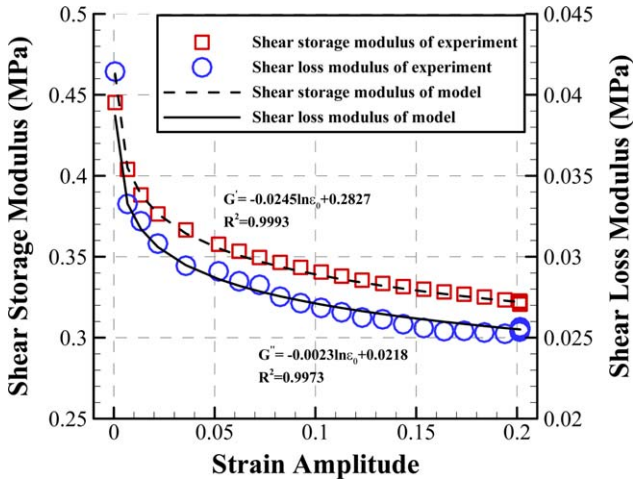

Figure 9. Strain amplitude dependence of shear storage and shear loss moduli for ASR. [Color figure can be viewed in the online issue, which is available at wileyonlinelibrary.com.]

Table III. Coefficients for Silicone Rubber in eq. (4)

Modulus	k	b	R^2
G'	−0.0245	0.2827	0.9993
G''	−0.0023	0.0218	0.9973

In addition, it can be seen from Figures 7 and 8 that the storage modulus and the loss modulus decrease speedily within two temperature regions: (i) from −50 to −40°C, (ii) from −120 to −110°C. The reason for that phenomenon is that the two transition temperatures are in or close to these two temperature regions.

The strain amplitude sweep test (5 Hz, 20°C) was carried out with the double shear deformation mode. The dependences of the shear storage modulus and the shear loss modulus on the strain amplitude were shown in Figure 9. It is easy to be observed that there is a nonlinear relationship between the shear storage modulus (or the shear loss modulus) and the strain amplitude. After having tried many types of functions, the following formula is found to be suitable for describing the relationships between the shear modulus G (including the shear storage modulus G' and the shear loss modulus G'') and the strain amplitude ε_0:

$$G = k \ln \varepsilon_0 + b \tag{4}$$

where k and b are the model parameters. The shear modulus decreases with the increment of strain amplitude: from 0.445 to 0.32 MPa for G' and from 0.042 to 0.025 MPa for G''. The fitted model coefficients and R^2 for G' and G'' are illustrated in Table III. As depicted in Table III, the nonlinear model has a well agreement with the experimental data of the strain amplitude sweep test. So, the moduli of the ASR have an apparent nonlinear dependence on the strain amplitude, as shown by eq. (4).

CONCLUSIONS

In the present work, the aerospace-level ASR was prepared and the mechanical properties were investigated through the hyperelastic measurements, the dynamic mechanical tests and the rheological experiments. The hyperelastic analysis shows that (i) the tensile strength and the break strain of the ASR are separately 3.00 MPa and 281%, and (ii) the proposed model exhibits good descriptions of the uniaxial tension and the simple compression behaviors of the ASR. The dynamic mechanical analysis indicates that (i) two transition temperatures (one lying between −50 and −35°C relates to the crystallization transition and the other of −115°C relates to the glass transition) are observed for the ASR, (ii) within two temperature intervals ([−120°C, −110°C] and [−50°C, −40°C]), the storage modulus and the loss modulus decrease quickly, and (iii) the storage modulus, the loss modulus and the loss factor (larger than

0.24) become stable when the temperature is higher than −35°C. The rheological analysis presents that (i) at the temperature of −120°C and −110°C, with increasing frequency, storage modulus and loss modulus appeared an obvious growth, (ii) the moduli of the ASR have an apparent nonlinear dependence on the strain amplitude, and (iii) a nonlinear function is utilized to express the relationship between the shear modulus and the strain amplitude and this nonlinear model shows well agreements with the experimental data. Summing up, the ASR has stable elastic and damping properties above −35°C and could be widely used in industrial applications. The investigations on the aerospace-level ASR in this paper have some meanings for its usage in aerospace products. The studies on the crossing linking density, mixing ratio, etc will be carried out in our future work.

REFERENCES

1. Nunes, L. C. S. *Mater. Sci. Eng. A* **2011**, *528*, 1799.
2. Podnos, E.; Becker, E.; Klawitter, J.; Strzepa, P. *J. Biomech.* **2006**, *39*, 1217.
3. Misra, R. D. K.; Yuan, Q. *Mater. Sci. Eng. C* **2012**, *32*, 902.
4. Yu, L. J.; Liu, S. L.; Ye, L. M.; Huang, G. S.; Xu, Y. T. *J. Wuhan Uni. Technol. Mater. Sci. Ed.* **2012**, *1*, 130.
5. Tan, J. Z.; Chao, Y. J.; Li, X. D.; Van Zee, L. W. *J. Power Sources* **2007**, *172*, 782.
6. Wang, Y. B.; Huang, Z.; Zhang, L. *Trans. Nonferrous Met. SOC. China.* **2006**, *16*, 517.
7. Crawford, B.; Doherty, A. P.; Spedding, P. L.; Herron, W.; Proctor, M. *Asia-Pacific J. Chem. Eng.* **2010**, *5*, 882.
8. Kulik, V. M.; Boiko, A. V.; Bardakhanov, S. P.; Park, H.; Chun, H. H.; Lee, I. *Mater. Sci. Eng. A* **2011**, *528*, 5729.
9. Zhou, Y. X.; Wang, J. Y.; Chen, H. H.; Nie, Q.; Sun, Q. H.; Wang, Y. S. *J. Electrostat.* **2009**, *67*, 422.
10. Hao, L.; Shi, Z.; Zhao, X. *React. Funct. Polym.* **2009**, *69*, 165.
11. Chen, D. Z.; Nie, J. R.; Yi, S. P.; Wu, W. B.; Zhong, Y. L.; Liao, J.; Huang, C. *Polym. Degrad. Stab.* **2010**, *95*, 618.
12. Tijing, L. D.; Park, C.-H.; Kang, S.-J.; Amarjargal, A.; Kim, T.-H.; Pant, H. R.; Kim, H. J.; Lee, D. H.; Kim, C. S. *Appl. Surf. Sci.* **2013**, *264*, 453.
13. Machado, G.; Chagnon, G.; Favier, D. *Mech. Mater.* **2012**, *50*, 70.
14. Wang, X. Y.; Xia, Z. D.; Yuan, B.; Zhou, H.; Li, Z.; Chen, N. N. *Mater. Des.* **2013**, *51*, 287.
15. Loew, R.; Meier, P. *Finite Elem. Anal. Des.* **2007**, *43*, 453.
16. Davidson, J. D.; Goulbourne, N. C. *J. Mech. Phys. Sol.* **2013**, *61*, 1784.
17. Dias, V.; Odenbreit, C.; Hechler, O.; Scholzen, F.; Ben Zineb, T. *Int. J. Adhes. Adhes.* **2014**, *48*, 194.
18. Meunier, L.; Chagnon, G.; Favier, D.; Orgeas, L.; Vacher, P. *Polym. Test.* **2008**, *27*, 756.
19. Renaud, C.; Cros, J.-M.; Feng, Z.-Q.; Yang, B. T. *Int. J. Imp. Eng.* **2009**, *36*, 659.
20. Khajehsaeid, H.; Arghavani, J.; Naghdabadi, R. *Eur. J. Mech. A/Sol.* **2013**, *38*, 144.
21. Lopez-Pamies, O. C. R. *Mecanique.* **2010**, *338*, 3.
22. Chiu, H.; Chiu, S.; Wu, J. *J. Appl. Polym. Sci.* **2003**, *89*, 959.
23. Wang, Y. P.; Fang, L. M.; Xu, C. H.; Chen, Z. H.; Chen, Y. K. *Polym. Test.* **2013**, *32*, 1072.
24. Wang, Y. P.; Fang, L. M.; Xu, C. H.; Chen, Z. H.; Chen, Y. K. *J. Appl. Polym. Sci.* **2014**, *131*, 39945.
25. Rey, T.; Chagnon, G.; Le Cam, J.-B.; Favier, D. *Polym. Test.* **2013**, *32*, 492.
26. Guelon, T.; Toussaint, E.; Le Cam, J.-B.; Promma, N.; Grediac, M. *Polym. Test.* **2009**, *28*, 715.
27. Meng, Y.; Wei, Z.; Lu, Y. L.; Zhang, L. Q. *eXPRESS Polym. Lett.* **2012**, *11*, 882.
28. Vesenjaka, M.; Krstulovic-Opara, L.; Ren, Z. *Polym. Test.* **2012**, *31*, 705.
29. Li, B.; Chen, S.; Zhang, J. *J. Appl. Polym. Sci.* **2014**, *131*, 39708.
30. Moghadam, M. K.; Morshedian, J.; Ehsani, M.; Laine, R. M.; Kuang, L. Y.; Umehara, N. *IEEE Trans Dielectr. Electr. Insul.* **2014**, *1*, 244.
31. Weia, Y. T.; Nasdala, L.; Rothert, H.; Xie, Z. *Polym. Test.* **2004**, *23*, 447.
32. Ramorino, G.; Vetturi, D.; Cambiaghi, D.; Pegoretti, A.; Ricco, T. *Polym. Test.* **2003**, *22*, 681.
33. Shit Pathik Shah, S. C. *Natl. Acad. Sci. Lett.* **2013**, *4*, 355.
34. Zhang, T. F.; Mao, Y. J.; Chen, D. Z.; Wu, W. B.; Yi, S. P.; Mo, S. B.; Huang, C. *Polym. Degrad. Stab.* **2013**, *98*, 916.
35. Li, S. L.; Cao, G. Q.; Yang, C.; Sun, P. D. *China Surfactant Detergent Cosmetics.* **2014**, *6*, 324.
36. White, J. R.; De, S. K. Rubber Technologist's Handbook; Smithers Rapra Technology: United Kingdom, **2001**.
37. Bradley, G. L.; Chang, P. C.; McKenna, G. B. *J. Appl. Polym. Sci.* **2011**, *81*, 837.
38. Holzapfel, G. A. Nonlinear Solid Mechanics: A Continuum Approach For Engineering; Wiley, **2008**.
39. Treloar, L. R. G. The Phyiscs of Rubber Elasticity; Oxford University Press: United Kingdom, **2005**.
40. Mlyniec, A.; Morawska-Chochol, A.; Kloch, K.; Uhl, T. *Polym. Degrad. Stab.* **2014**, *99*, 290.
41. Shaw, M. T.; MacKnight, W. J. Introduction to Polymer Viscoelasticity; Wiley, **2005**.
42. Dick, J. S. Rubber Technology: Compounding and Testing for Performance; Hanser Gardner Pubns: Cincinnati, OH, **2009**.